JP1J.11 **IMPACT OF RADAR DATA ASSIMILATION ON STORM PREDICTIONS USING A MESOSCALE MODEL**

Mei Xu[1], N. Andrew Crook, Yubao Liu and Roy Rasmussen
National Center for Atmospheric Research[2], Boulder, Colorado

1. INTRODUCTION

High resolution mesoscale models, such as MM5, are potentially useful tools for predicting the initiation, evolution and decay of severe storms in the 1-12 hour range. However, despite various improvements in model physics, there still exist significant discrepancies between the observations and model predictions of the timing, duration and amount of precipitation produced by the storms. To improve the accuracy of the MM5 forecasts, high resolution datasets need to be analyzed and assimilated into the model initial conditions.

The objective of this work is to test a real-time short-term forecasting system for aviation applications. The modeling framework was adopted from the real-time four-dimensional data assimilation and short-term forecasting system (RTFDDA) developed at NCAR (Cram et al., 2001; Liu et al., 2002). Built upon a high-resolution MM5 and an observational nudging (Newtonian relaxation) scheme, the system assimilates observations from various sources continuously and provides updated 3-dimensional analyses and short-term forecasts in a cycling fashion.

To enhance the system for aviation applications, a radar data assimilation component has been added to incorporate multi-radar observations. Techniques for assimilating radar observations into MM5 have been tested. In order to be more applicable to real-time operations, a less expensive method based on the grid nudging technique, is tested with RTFDDA. The radar data ingested are the real-time Level II radar observations made available via the Collaborative Radar Acquisition Field Test (CRAFT, Droegemeier et al., 2002) network and provided to us by National Severe Storm Laboratory (NSSL). Three-dimensional mosaic reflectivity for CONUS (Zhang et al., 2005), as well as radial velocity from the individual radars, are accessible in real-time.

The RTFDDA system with radar data assimilation was run in operational demonstrations during the winters of 2004 and 2005, and the summer of 2005. Preliminary results from the real-time tests are described. Some results from case studies are also presented in the paper.

2. RTFDDA WITH RADAR DATA ASSIMILATION

The RTFDDA system was initially developed for the Army as a quick cycling FDDA system to provide real-time local scale analyses and short term forecasts. The data assimilation engine of the RTFDDA system is based on observational nudging. Each observation is ingested into the model at the observed time and location, with tuned space and time weights. The system runs in three-hour cycling mode and is cold started once a week. Currently, traditional observations (rawinsonde, metar, ship and buoy reports), as well as non-traditional observations (mesonet, aircraft reports, profilers and satellite wind) are nudged in this manner.

A radar data assimilation scheme has been added to RTFDDA to ingest three-dimensional mosaic reflectivity data as well as the wind vectors derived from the radar radial velocity observations. To produce the mosaic reflectivity, reflectivity observations from the individual radars are mapped to a common Cartesian grid, and then combined to form a unified 3D reflectivity field (Zhang et al., 2005). The grid resolution of the mosaic reflectivity is 1 km in the horizontal and 0.5 -1 km in the vertical. The datasets are updated every 5 minutes. The volume-velocity processing (VVP) method is used to derive full wind vectors from single radar radial velocity observations at a reduced spatial resolution. The technique divides radar sweeps into small volumes for which the wind parameters are estimated by multivariate regression analysis.

A grid nudging scheme is used to assimilate the mosaic reflectivity data. The mosaic reflectivity is first converted to 3D precipitation field and interpolated to the model grid. Then the precipitation field, together with the corresponding latent heat, are nudged on the inner meshes. The data insertion are performed at an interval of 30 min. on the 10 km grid and 15 min. on the 3.3 km grid. The scheme also includes an algorithm for adjusting the humidity according to radar observations. The nudging parameters can be tuned to optimize data effect on the model forecasts. A relatively large coefficient is used on the 3.3 km grid in the summer operation. Due to the fact that CPS is employed on the 10 km grid, a smaller nudging coefficient is used.

---

1 Corresponding author address: Mei Xu, NCAR/RAP, P.O.Box 3000, Boulder, Colorado 80307. Email: meixu@ucar.edu

2 The National Center for Atmospheric Research is sponsored by the National Science Foundation.

The VVP wind vectors can be assimilated into RTFDDA using observational nudging. The VVP estimates are dependent on the size of the analysis volume. The optimal analysis volume size may vary from case to case. An analysis volume of 30° in azimuthal width and 25 km in range extent is used in our real-time tests. The assimilation schemes for mosaic reflectivity and VVP wind vectors are independent of each other and can be tested separately.

3. REAL-TIME TEST IN WINTER 2004

The RTFDDA system with radar data assimilation was tested during January 31 – March 19 of 2004. Only mosaic reflectivity data in the Corridor Integrated Weather System (CIWS) NE domain were ingested. The system was run in parallel to an operational RTFDDA at the Army's Aberdeen Testing Center in Maryland. The same model grid configuration (Fig. 1 - triply nested grid with resolution of 3.3 km, 10 km and 30 km) and physics options were used in the parallel and operational runs. The fine mesh centers near the Baltimore / Washington International Airport (BWI), and the La Guardia Airport (LGA) is covered by the 10 km grid. The observations used in each cycle of the operational run (dubbed Control run hereafter) were duplicated and used in the parallel run (dubbed Parallel run). The only difference between the parallel and control runs was the mosaic radar reflectivity data assimilated in the parallel run.

Five major storm events and several smaller storms were recorded in the domain during the period. The RTFDDA run was stable, although there were short, intermittent breaks in the radar data flow. For each 3 h cycle, a 3-h data assimilation and 9-h forecast were performed in the parallel run. The rain/snow mixing ratio field (derived from radar reflectivity) was nudged and a fraction of the latent heat associated with the mixing ratio field was added to the model during the data assimilation period. No water vapor adjustment was done in the real-time demonstration experiment.

Statistical verification has been performed for the parallel and control runs for the entire demonstration period (20040131 – 20040319), as well as for the episodes when precipitation occurred in the model grid. Approximately 1/3 to 1/2 of the total hours of operation were characterized by some precipitation in the CIWS domain. Model analyzed and forecast fields of temperature, humidity, wind speed and wind direction are verified against surface and upper-air station observations on each domain. The precipitation fields are verified using radar observations as well as observations from tipping-bucket rain/snow gauges.

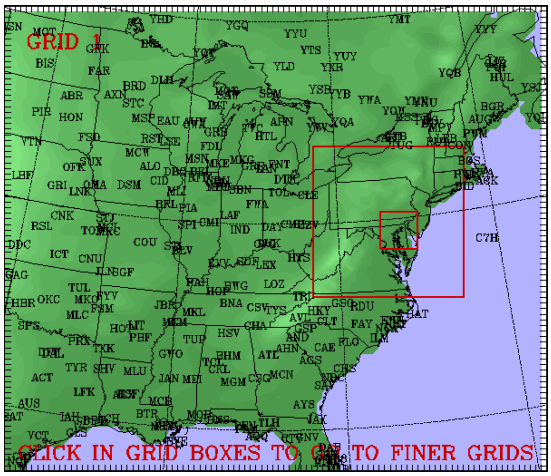

Fig. 1 The model grid used in RTFDDA for snowfall forecast in winter 2004.

Verification vs. surface station observations

Tables 1 gives the mean bias and rms errors of temperature, wind speed and wind direction from the parallel and control runs, verified against the surface station observations on the 3.3 km grid for the entire test period. Only the surface observations within 10 minutes of the model output time (hourly) are used in the verification. At each model output hour, approximately 20 observations in the inner grid are used in verification.

T (K)	Parallel Run		Control Run	
	Bias	**Rms**	**Bias**	**Rms**
Final	-0.19	1.36	-0.41	1.36
0-3 h fcst	-0.25	1.58	-0.60	1.74
3-6 h fcst	-0.41	2.01	-0.91	2.25
6-9 h fcst	-0.52	2.15	-1.07	2.44
Ws (m/s)	**Parallel Run**		**Control Run**	
	Bias	**Rms**	**Bias**	**Rms**
Final	0.12	2.00	0.11	1.74
0-3 h fcst	0.31	2.26	0.17	1.93
3-6 h fcst	0.21	2.51	0.21	2.32
6-9 h fcst	0.23	2.53	0.21	2.34
Wd (degree)	**Parallel Run**		**Control Run**	
	Bias	**Rms**	**Bias**	**Rms**
Final	4.47	33.50	3.69	32.43
0-3 h fcst	4.61	38.32	3.62	37.37
3-6 h fcst	5.56	42.77	4.96	42.75
6-9 h fcst	5.48	43.90	4.05	43.79

Table 1. Verification statistics for surface temperature (T), wind speed (Ws) and direction (WD) during 20040131 – 20040319.

It is found that the parallel run produces surface temperature fields that agree better with observations, especially during the forecast stage. On the other hand, it gives larger statistical errors in the wind speed and direction fields than the control run. As the reflectivity data are nudged, the model thermal fields are improved through more accurate specifications of the microphysical and radiative processes. Table 1 shows that this improvement of temperature carries through the forecast period. On the other hand, the radar data assimilation may have induced some small-scale circulations that do not agree well with the surface observations, thus degrading the wind verification. A verification of the model wind field with the radar radial velocity data will be done later.

The diurnal cycle of the verification statistics (Figure 2) indicates that the improvement in temperature verification and the error increase in wind verification do not depend on the hour of the day. In fact, the verification for individual storm cases shows that the impact of radar data is more dependent on the stage of the storm. A larger improvement in temperature verification is seen during stronger precipitation period.

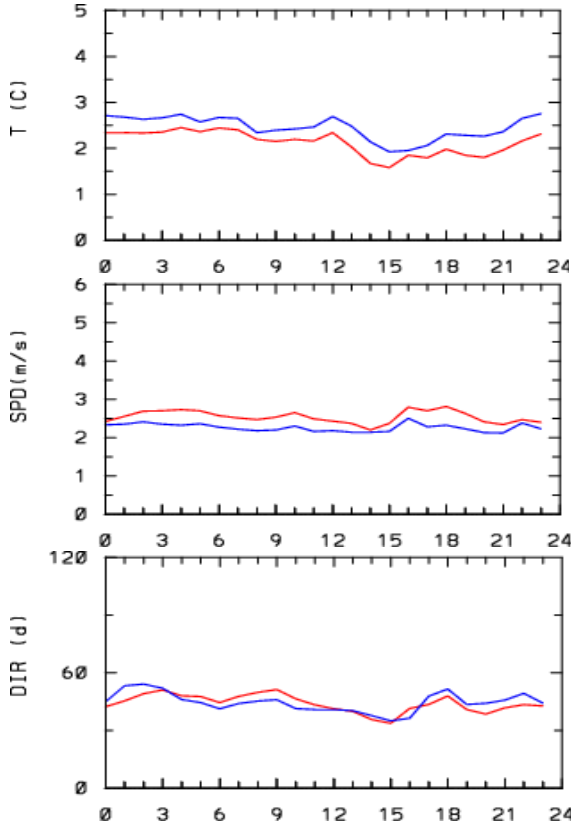

Figure 2 RMS errors in the 6-9 h forecast of T, Ws and Wd. Each value is a 7 week-long average for the hour of the day. Red: Parallel run with radar data nudging. Blue: the control atc operational run.

Verification of the precipitation field

The 3D snow mixing ratio (qr), as well as the ground precipitation from model grid 2 and 3 are verified using the radar observations. Please note that the original radar data have a higher spatial and temporal resolution than the qr data that are actually assimilated into the model. Figure 3 shows the mean RMS error and correlation coefficient between the modelled and radar observed qr fields, as a function of the forecast hour. The verification is only done for the cases when a moderate level of qr is observed and in the area where radar observations are available.

Due to unexpected computer problems, the original MM5 output of forecasts from the control ATC operational run were not archived. Only the final analyses and verification pairs were saved. Therefore, on Figure 3, the qr verification from the control run is only valid for the analysis period. The short-term forecasts from these operational analyses typically have a similar or slightly less skill for precipitation forecast, so the qr verification of the final analysis of the control run may be viewed as the baseline skill in precipitation forecasting by the operational RTFDDA.

Figure 3 shows that the prediction skills of the parallel run for the precipitation field decrease rapidly with forecast time. In the final analyses (data assimilation period), the modeled qr field follows the radar observations relatively well, as indicated by the

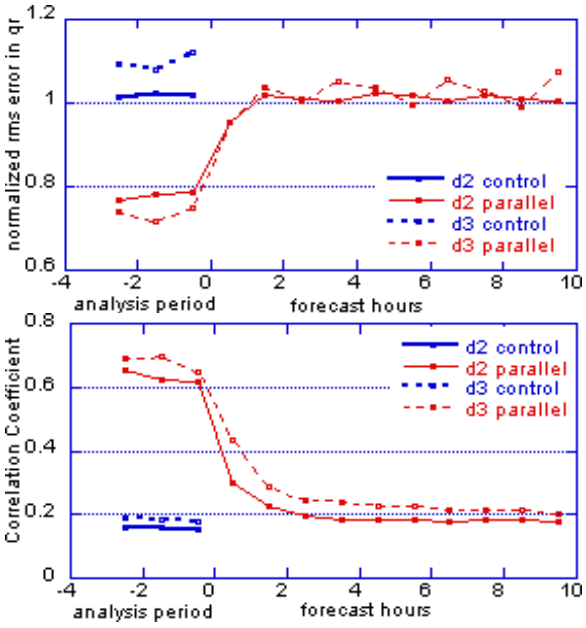

Figure 3 The RMS error and the correlation coefficient between the modelled and radar observed qr fields for the control run (blue) and parallel run (red), verified on model grid 2 (solid) and 3 (dashed).

relatively high levels of correlation coefficient. The correlation coefficient also shows improved qr forecasts within 3 h after the data assimilation. However, little impact of radar data is seen in the 3D qr field 3 hours after the data assimilation,

The qr verification demonstrates the usefulness of the radar data nudging scheme in blending the qr observations into the model analyses, and in improving the skills for 0-3 h forecasts. Little improvement by radar data is seen in qr forecasts beyond 3 hours.

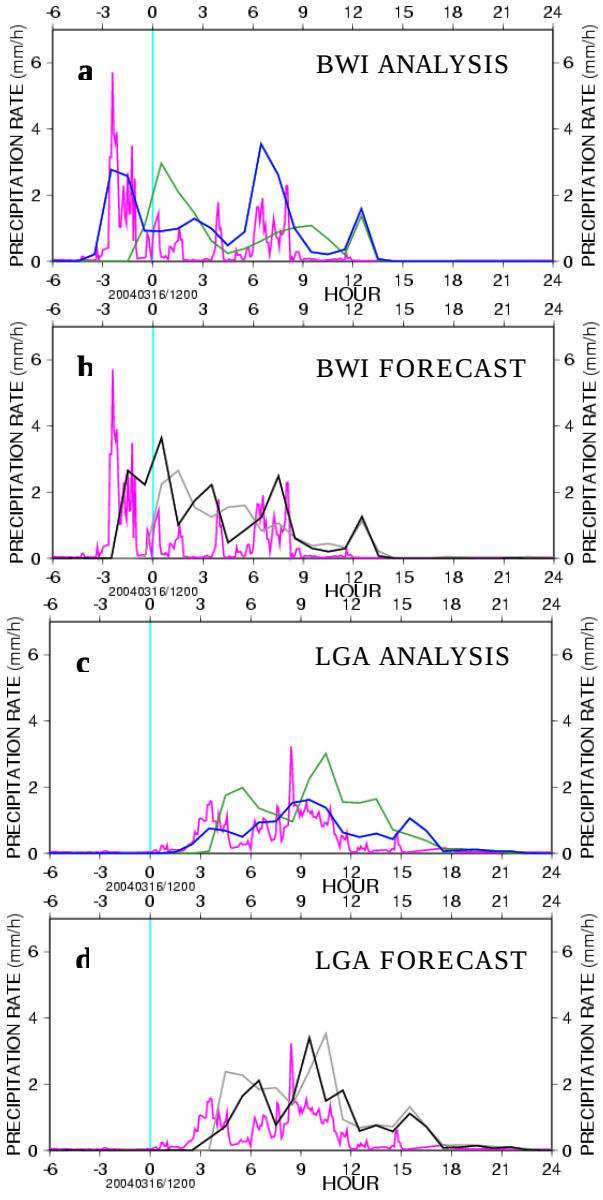

Fig. 4 Precipitation rates at BWI (a, b) and LGA (c, d) during the March 16, 2004 snowstorm event. Pink: radar observation. Green: RTFDDA analysis without radar data. Blue: RTFDDA analysis with radar data. Black: 1-3 h forecast from RTFDDA with radar data. Grey: 4-6 h forecast from RTFDDA with radar data.

Snowfall forecast at the airports: An example

A snowstorm occurred in the Northeast on March 16, 2004. The snowfall rates at BWI and LGA from the parallel run (RTFDDA with radar data assimilation) are plotted in Figure 4. Also plotted are the snowfall from final analysis of the control run. The radar data of precipitation rate at the two airports are derived from the lowest level reflectivity, and have a frequency of 5 minutes.

At both airports, the onset of precipitation in the control analyses lags behind the observation by 1-2 hours. The analysis field in the parallel run follows the observed trend very well, and shows improvement over the control analysis. There is still some positive impact from the radar data in the 0-3 h forecasts. The 3-6 h forecasts show no evident improvement of skills.

The temporal variations in model output are rather smooth. This is probably due to the smoothing effect of the model, as well as to the hourly output frequency. The performance of the system at the airports for this case is typical of its forecast skills for airport snowfall during the multi-week demonstration.

4. EFFECT OF VVP WIND VECTORS

The RTFDDA with radar data assimilation was again operational during the winter of 2005, for a domain centered in the OHARE Internation Airport, Chicago, Illinois. The effect of assimilating VVP wind vectors in addition to assimilating mosaic reflectivity has been examined during two winter storm events, occurred on January 12-13 and January 19, 2005, respectivity. The first storm was associated with relatively strong large-scale forcing, while the second storm had more local convective structures.

For the January 12-13 storm, the VVP wind vectors slightly improve the forecast timing of the snowfall in OHARE. Figure 5 shows that the forecast position of the strongest snowband at 06 Z of January 13 is further downstream in the experiment assimilating VVP wind than in the reflectivity-only and no-radar runs. The radar observations show that the strongest band had already passed the lake (not shown) by 06 Z. However, no systematic improvement by the VVP wind is seen in the verification of the forecast temperature and wind fields. A further examination show that many VVP wind vectors are rejected by the model because they differ too much from the model values. This is especially true for the case of January 19, 2005 in which no significant impact of VVP wind assimilation is seen.

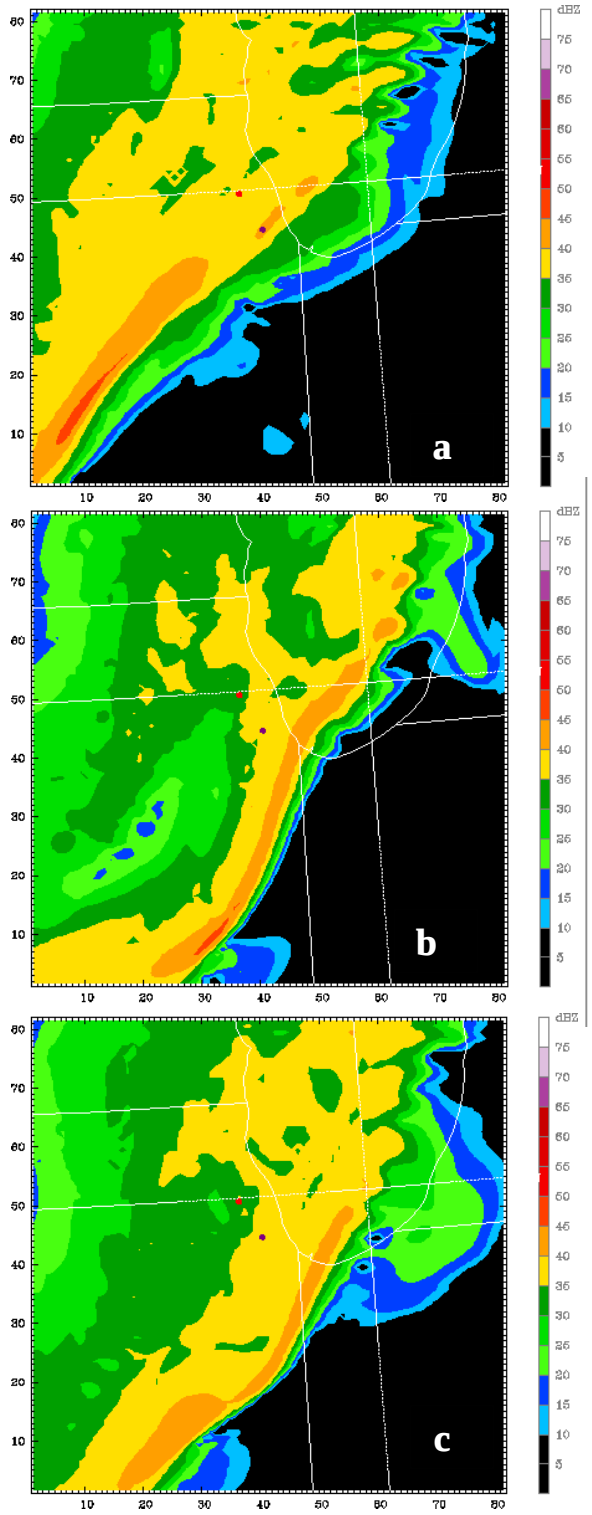

Fig. 5 Simulated reflectivity fields for 06 Z of January 13, 2005, forecast by the 02 Z cycle (4 h forecasts). (a) RTFDDA forecast without radar data assimilation. (b) RTFDDA with reflectivity assimilation. (c) RTFDDA forecast with radar reflectivity and VVP wind.

5. EFFECT OF REFLECTIVITY AND LATENT HEAT IN A SUMMER CONVECTIVE STORM EVENT

The model is tested for summer storm predictions in case studies for summer 2004 and in a real-time test in summer 2005. The model forecasts are used to provide environmental conditions for the NCAR Autonowcast system (Cai el al., 2005), and the overall skills are compared with skills of forecasts from other short-term forecasting methods (Wilson et al., 2005).

Case studies show that the reflectivity nudging, specifically, the latent heat adjustment, can have a significant impact on the organization and evolution of the storm. For example, in the case of July 13, 2004 squall line storm, a single strong cell initiated in northern Illinois at 16-17 Z, and grew into a large squall line storm in southern Indiana a few hours later. Without radar data assimilation, the forecast initiation is about 1-2 hours later than the observed and location of the initial cell is about ~60 km to the south of the observed. The forecast convective cells in the mature stage of the storm are more scattered, and mostly located in northern Indiana instead southern Indiana as the observed (Figure 6a,c). When the latent heating is modfied with the precipitation field, the initial cell is enforced in the correct location, which suppresses the wrong cell growth in the model. Station verifications reveal that the surface temperature forecast after the radar data assimilation agrees better with the surface observations. The result is a more significant cold pool and altered storm track (Figure 6b). The effect of reflectivity and latent heat nudging may vary for different types of summer storms. A systematic evaluation of the impact of radar data assimilation on summer storm forecasting is yet to be conducted after the real-time test is finished.

6. SUMMARY

A MM5 based system was tested for short-term forecasting of storms. A radar data assimilation scheme based on nudging was employed for assimilating Level II data from multiple radars. Data processing and ingest modules were developed to make use of the mosaic reflectivity and radial velocity datasets. The system was designed to run efficiently in real-time.

Effect of assimilating Level II radar reflectivity is evaluated in a winter real-time run, which demonstrates the usefulness of the radar data nudging scheme in blending the qr observations into the model analyses, and in improving the skill for 0-3 h precipitation forecasts. However, nudging reflectivity produces little improvement in qr forecasts beyond 3 hours.

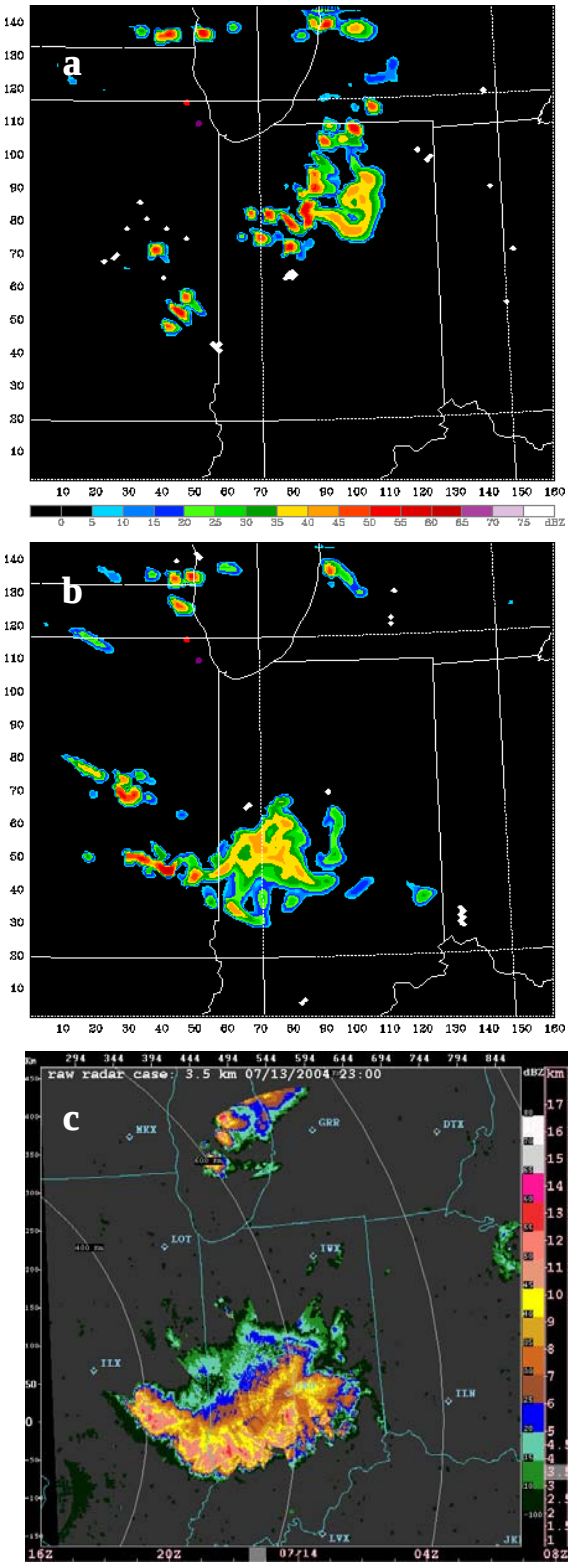

Fig. 6 Reflectivity fields at 23 Z of July 13, 2004. (a) 3-h RTFDDA forecast without radar data assimilation. (b) 3-h RTFDDA forecast with reflectivity (and latent heat) assimilation. (c) radar observations.

Case studies of winter storms show that nudging VVP wind vectors may improve the forecasting of snowband location. However, additional processing is required in order for the wind vectors to be used through observational nudging.

Case studies of summer storms show the reflectivity and latent heat nudging scheme may help improve the 1-6 h forecasting of convective storms. A systematic evaluation of the effect of radar data assimilation will be conducted in a 3-month-long summertime real-time test.

ACKNOWLEGEMENT

This research is funded by the Federal Aviation Administration (FAA) and Army Testing and Evaluation Command (ATEC).

Cai, H., and coauthors, 2005: Impacts of MM5 model data on the performance of the NCAR Auto-Nowcast system. Paper 6R.3, 32nd Conference on Radar Meteorology. Albuquerque, NM. 24-29 October, 2005. AMS.

Cram, J., and coauthors, 2001: An operational mesoscale RT-FDDA analysis and forecasting system. Preprints, 18th WAF and 14th NWP conferences. Ft. Lauderdale, Florida. 30 July-3 August, 2001. AMS.

Droegemeier, K., K. Kelleher, et al., 2002: Project CRAFT: A test bed for demonstating the real-time acquisition and archival of WSR-88D base (Level II) data. Preprints, 18th Int. Conf. Meteor. Ocean. Hydrology, Orlando, Florida. AMS.

Liu, Y., and coauthors, 2002: Performance and enhancement of the NCAR/ATEC mesoscale FDDA and forecasting system. Preprints, 15th Conference on Numerical Weather Prediction. San Antonio, Texas. 10-16 August, 2002. AMS.

Wilson, J. W. and coauthors, 2005: Experiments in very short period forecasting of convective storms using radar extrapolation and numerical weather prediction methods. Paper J1J.6, 32nd Conference on Radar Meteorology. Albuquerque, NM. 24-29 October, 2005. AMS.

Zhang, J, K. Howard, J.J. Gourley, 2005: Constructing three-dimensional multiple-Radar reflectivity mosaics: Examples of convective storms and stratiform rain echoes. Journal of Atmospheric and Oceanic Technology, 22, 30-42.